Evolution of sensory systems underlies the emergence of predatory feeding behaviours in nematodes

Marianne Roca[1], Güniz Göze Eren[1], Leonard Böger[1,2], Olena Didenko[1], Wen-sui Lo[3], Monika Scholz[2] & James W. Lightfoot[1*]

1. Max Planck Research Group Genetics of Behavior, Max Planck Institute for Neurobiology of Behavior - caesar, Bonn, Germany.
2. Max Planck Research Group Neural Information Flow, Max Planck Institute for Neurobiology of Behavior – caesar, Ludwig-Erhard-Allee 2, 53175, Bonn, Germany.
3. Northwest A&F University, Yangling, Shaanxi, 712100, China.

* corresponding author

Abstract

Understanding how animal behaviour evolves remains a major challenge, with few studies linking genetic changes to differences in neural function and behaviour across species. Here, we identify specific sensory adaptations associated with the emergence of predatory feeding behaviours in the nematode *Pristionchus pacificus.* While *Caenorhabditis elegans* uses contact-dependent sensing primarily to avoid threats, *Pristionchus pacificus* has co-opted this modality to support both avoidance and prey detection, enabling context-dependent predatory behaviour. To uncover a potential mechanism underlying the evolution of *P. pacificus* prey perception, we mutated 27 canonical mechanosensory genes and assessed their function using behavioural assays, automated behavioural tracking, and a machine learning analysis of behavioural states. While several mutants showed mechanosensory defects, *Ppa-mec-6* mutants specifically also impaired prey detection, indicating the emergence of a novel mechanosensory module linked to predatory behaviour. Furthermore, disrupting both mechanosensation alongside chemosensation revealed a synergistic influence for these modalities. Crucially, both mechanosensation and chemosensation pathways converge in the same environmentally exposed IL2 neurons, and silencing these cells induced severe predation defects validating their importance for prey sensing. Thus, predation evolved through the co-option of mechanosensory and chemosensory systems that act together to shape the evolution of complex behavioural traits.

Introduction

Sensory systems represent the primary mechanism through which an organism acquires environmental information. These signals can be used for finding food, avoiding predators, detecting mates,

and navigating through complex surroundings. Detecting these environmental cues is dependent on specialised sensory systems which are often finely tuned to specific stimuli. Crucially, these systems are not static and their modification can profoundly affect the evolutionary trajectory of a species (1). Mechanisms of sensory system evolution include modifications to receptors, such as changes to receptor selectivity or sensitivity, as well as associated gene losses or gains (1). Examples of such events have been observed in several invertebrate species with changes in receptor function influencing feeding ecology in fruit flies (2), mosquitoes (3), and cockroaches (4). Similarly, in vertebrates, changes to sweet receptors have modified the feeding behaviours of songbirds and bats (5, 6) while in deep sea fish, a greatly expanded number of opsins has evolved to maximise their visual sensitivity in minimal light environments (7). Thus, sensory system evolution shapes the behavioural repertoire of an organism and facilitates its adaptation to its ecological niche.

In nematodes, a remarkable range of behaviours has evolved in accordance with the diverse ecologies found across the phyla. In particular, with their exceptional array of genetic and molecular tools, (8–10) alongside their distinct feeding ecologies, *Caenorhabditis elegans* and *Pristionchus pacificus* represent a powerful interspecies system for understanding the evolutionary adaptations influencing sensory perception. More specifically, while *C. elegans* is a microbial feeder, *P. pacificus* is an omnivorous species and not only feeds on bacteria but is also a predator of other nematodes (11). This expanded feeding behaviour is linked to a mouth-form plasticity with *P. pacificus* nematodes capable of developing one of two morphs. These are either the stenotomatous (st) or eurystomatous (eu) form. The st mouth is narrow with a single tooth and only permits bacterial feeding or scavenging, whereas the eu mouth is wider and possesses an additional tooth which facilitates both bacterial feeding and predation (11). Furthermore, predatory behaviour is directed towards not only other nematode species but also con-specifics. However, closely related strains are spared due to the presence of a robust kin-recognition system (12, 13). Crucially, how sensory systems evolved to accommodate the predatory behaviours is an open question.

In *C. elegans,* bacterial food is detected through well described foraging behaviour using their chemosensory and texture sensing systems (14, 15). In *P. pacificus*, little is known of its food and prey sensing mechanisms, however, they show specific sensory adaptations relevant to their ecology. In particular, *P. pacificus* are attracted to many bacterial species found concurrently in their environment and are also attracted to specific insect pheromones as *Pristionchus* are frequently found associated with scarab beetles (16). During food sensing and foraging, *P. pacificus* transitions between the docile bacterial feeding and aggressive predatory feeding states through the internal balance of octopamine and tyramine. These neuromodulators act on a group of head sensory neurons expressing the corresponding receptors (17). Contact between the nose of the predator and the surface of the prey during aggressive predatory bouts can

68 initiate the activity of their movable tooth to puncture through the cuticle of the prey (11, 18, 19). However,
69 the precise stimuli responsible for detecting prey contacts are currently unknown.
70 Here, to understand how the *P. pacificus* sensory systems have contributed to the emergence of
71 predatory feeding we have investigated the role of mechanosensory adaptations for these behaviours. Using
72 a candidate-based approach, we identified a crucial role for mechanosensation in predation. We find *Ppa-*
73 *mec-6* is necessary for this process and may contribute to these behaviours through a previously undescribed
74 predatory-associated mechanosensory channel. Furthermore, we demonstrate that mechanosensation is
75 required alongside chemosensory inputs and that these acts synergistically to execute efficient predation
76 behaviours. We also reveal that chemosensory and mechanosensory components are expressed in the same
77 externally projecting and environmentally exposed neurons, indicating functional convergence into the
78 same sensory circuits. Finally, we show that the functional inhibition of these neurons indeed disrupts
79 predation.
80

81 ## Results

82 ### Mechanosensation is involved in prey detection

83 *P. pacificus* is a voracious predator of other nematode larvae including *C. elegans* and this feeding
84 behaviour requires contact between predator and prey (Fig. 1A). Accordingly, we investigated the
85 importance of *P. pacificus* mechanosensation for detecting prey and a potential role in the evolution of its
86 predation behaviours. *Cel-mec-3* is critical transcription factor involved in the development and function
87 of mechanosensory neurons in *C. elegans,* and animals with mutations in this gene fail to respond to tactile
88 stimuli (20). In *P. pacificus,* using a *Ppa-mec-3* transcriptional reporter, we observed expression in several
89 neurons with similar cell body placements to the *C. elegans* mechanosensory neurons FLP, AVM, ALM,
90 PVM, PVD, and PLM (Fig. 1B), (20–22). To assess its role in mechanosensation in *P. pacificus,* we
91 generated a mutation in the *Ppa-mec-3* orthologue using CRISPR/Cas9. Similar to *C. elegans*, we found
92 *Ppa-mec-3* mutants fail to react to several classic mechanosensory assays including harsh touch, gentle
93 touch, and nose touch assays (Fig. 1C-E). Taken together, this indicates a conserved role for *Ppa-mec-3*
94 between species. Next, to assess a potential role for *Ppa-mec-3* in predatory feeding, we performed
95 previously established corpse assays (11). In corpse assays, starved *P. pacificus* adults are placed on a plate
96 saturated with *C. elegans* larval prey and predation success is determined by the number of corpses after a
97 designated time interval (supplementary Fig. 1A). Here, *Ppa-mec-3* predators show a significant reduction
98 in killing ability, with fewer larval corpses generated by predators than observed in control assays with
99 wildtype predators (Fig 1F). Thus, mechanosensory systems have acquired additional functions in *P.*
100 *pacificus* and are necessary for efficient prey detection.
101

102 **Mechanosensory genes have diversified across evolution**

103 Having established the importance of mechanosensation for predation, we next explored the
104 conservation of mechanosensory gene networks across nematode evolution. Frequent gene losses and gains
105 are observed between nematode species and this can be associated with novel evolutionary processes (23).
106 Therefore, we initially conducted a bioinformatic study of the mechanosensory systems across 8 nematode
107 species to investigate the evolution of this sensory modality across the nematode phyla (Fig. 2A). Our
108 analysis consisted of the two free-living species *C. elegans* and *P. pacificus* belonging to clade 5 as well as
109 several obligate parasite species of both plants and animals (23). We included orthologues of the *C. elegans*
110 predicted mechanostransduction channels belonging to the degenerin–epithelial Na+ channels
111 (DEG/ENaC) and transient receptor potential (TRP) gene families (22). We also included other known
112 mechanosensory genes such as *mec-6*, a paraoxonase-like protein which acts as a chaperone to ensure
113 channel function (24), and *pezo-1,* due to its reported role in food sensation (25). Compared to free-living
114 nematodes*,* parasitic nematodes frequently had a lower number of genes encoding mechanotransduction
115 channels, perhaps indicative of adaptations to their specific lifestyle. In contrast, comparisons between the
116 free-living nematodes *C. elegans* and *P. pacificus* generally showed a similar representation of gene
117 families with a few exceptions (Fig. 2A). These include the four *trpl* genes which are specific to *C. elegans*
118 but absent in other species including *P. pacificus* (22). Additionally, there are two large gene expansions in
119 *P. pacificus* among the DEG/ENaC gene family with five copies of *deg-1* in *P. pacificus* compared to one
120 in *C. elegans* and 11 *egas* genes in *P. pacificus* compared to four in *C. elegans*. Little is known regarding
121 the function of *egas* in *C. elegans* and many of the *P. pacificus egas* paralogues lack RNA-seq data to
122 validate their expression (10). However, *deg-1* has been shown in *C. elegans* to be required for the induction
123 of mechanoreceptor current in the sensory ASH neuron (26). Therefore, mechanosensory gene networks
124 appear relatively stable between *C. elegans* and *P. pacificus* but are more stochastic in parasitic nematodes
125 with their more complex life-styles and host interactions.

126 With the identification of genes potentially acting as mechanosensory channels in *P. pacificus,* we
127 conducted a candidate-based approach to identify components necessary for efficient prey detection
128 through *P. pacificus* nose contact. Candidates were selected based on known mechanosensory phenotypes
129 in *C. elegans* together with further validation through available *P. pacificus* expression data (10, 27).
130 Accordingly, we selected genes to target by CRISPR/Cas9 which included both TRP and DEG/ENaC
131 families as well as other associated mechanosensory genes. We selected the DEG/ENaC channels *Ppa-*
132 *mec-4* and *Ppa-mec-10* as well as *Ppa-mec-6*. In *C. elegans, Cel-mec-4* and *Cel-mec-10* are both involved
133 in the gentle touch response (22, 28) and *Cel-mec-6* has been shown to directly interact with *Cel-mec-4* and
134 *Cel-mec-10* to aid the function and stability of this mechanosensitive channel (24, 29). We targeted *Ppa-*
135 *osm-9, Ppa-ocr-2* and *Ppa-trp-4* together as in *C. elegans* these genes have an additive effect reducing its

136 nose touch responsiveness (30). Only *P. pacificus* triple mutants for these genes were analysed. *C. elegans*
137 nose touch response also requires *Cel-delm-1* and *Cel-delm-2* which are expressed in glial cells (31).
138 However, we could not identify one-to-one orthologues for these two genes in *P. pacificus* as both
139 paralogous sequences are closer to each other than to either *Cel-delm* or *Cel-acd* genes. Therefore, these
140 were named *delm/acd* and we mutated both candidates in *P. pacificus*. In *C. elegans*, *Cel-del-7* and *Cel-*
141 *del-8* are DEG/ENaC ion channel family members, with the former involved in mechanotransduction (32).
142 However, there is only one paralogue in *P. pacificus,* which we mutated and named *Ppa-del-7/8*. We also
143 generated a quintuple mutant of all paralogues of DEG/ENaC *Ppa-deg-1,* and targeted the DEG/ENaC
144 potential proprioception genes *Ppa-del-1, Ppa-unc-8* and *Ppa-unc-105* (22, 33). To further represent the
145 TRP gene family, we included *Ppa-trp-1, Ppa-trp-2, Ppa-pkd-2, Ppa-cup-5* and *Ppa-trpa-1, which,* in *C.*
146 *elegans*, are expressed in many neurons and most have roles in mechanotransduction (30, 31, 34, 35).
147 Finally, we targeted the ionotropic glutamate receptor *Ppa-glr-1* due to its role in mediating excitatory
148 neurotransmission in touch receptor neurons (36), and *Ppa-pezo-1* due to potential roles in food sensing
149 (25). This resulted in 26 genes of interest, and we investigated two alleles for each of these genes, which
150 were predicted to cause loss-of-function mutations (Supplementary Table 1).
151

152 **MEC-6 is required for efficient *P. pacificus* predation**

153 Initially, we tested all of our mutants for mechanosensory defects using the three touch assays
154 adapted from previous *C. elegans* studies. These assays measure the animal response to harsh touch, gentle
155 touch, and nose touch (22). The majority of the *P. pacificus* mutants did not show mechanosensory deficient
156 phenotypes. However, *Ppa-mec-4, Ppa-mec-10,* and *Ppa-mec-6* showed mechanosensory defects similar
157 to those described in *C. elegans,* and also similar to those observed in *Ppa-mec-3,* resulting in a response
158 to touch only half the time or less (Fig. 2B-D and supplementary Fig. 1B-D). Furthermore, all four mutants
159 were also more lethargic than wildtype worms, phenocopying *C. elegans* mechanosensory mutants (28).
160 Thus, as in *C. elegans, Ppa-mec-4, Ppa-mec-10, Ppa-mec-3,* and *Ppa-mec-6* are required for touch
161 sensation in *P. pacificus*. While previous reports in *C. elegans* have not identified a role for harsh touch
162 sensation in *Cel-mec-4* (30), this discrepancy between the two species may stem from subtle species-
163 specific sensitivity differences. Next, we tested all of our mutants for defects in predation using the
164 previously described corpse assays. While the majority of mutants displayed wildtype levels of predation,
165 reduced killing was observed in *Ppa-mec-6* (Fig 2E and supplementary Fig. 1E). This is similar to the defect
166 observed in the *Ppa-mec-3* mutants (Fig. 1F). Importantly, no predatory defect was observed in *Ppa-mec-*
167 *4* or *Ppa-mec-10,* indicating that the predatory abnormality is not the consequence of a general
168 mechanosensory defect, but rather is specific to the function of *Ppa-mec-3* and *Ppa-mec-6.* In *C. elegans,*
169 *Cel-mec-6* is involved in the assembly and function of mechanosensory ion channels and interacts with *Cel-*

170 *mec-4* and *Cel-mec-10* to form ion channel complexes that are essential for mechanotransduction (24, 29).
171 Our data indicates that while the *Ppa-mec-4* and *Ppa-mec-10* channels are not required for prey detection
172 in *P. pacificus*, *Ppa-mec-6* may function as part of an additional, as yet unknown, mechanosensory ion
173 channel involved in detecting prey contact. Thus, specific mechanosensory inputs are necessary for prey
174 detection in *P. pacificus.* However, as predation is not fully abolished, additional sensory inputs also
175 contribute to prey detection ability.
176

177 **Mechanosensation and other predatory-associated traits**

178 Predation in *P. pacificus* is dependent on the formation of the eu mouth morph which is determined
179 by a multitude of environmental and genetic factors (37, 38). To assess if mechanosensation also influences
180 the mouth morph fate, we screened our mutant library for any effect on mouth form ratio. All mutants
181 showed wildtype levels of eu to st morphs (supplementary Fig. 2A and B). In addition, *P. pacificus* has a
182 robust kin-recognition mechanism which prevents attacks on its own progeny and close relatives, while
183 facilitating the cannibalism of other con-specific competitors (12, 13). Due to the prey detection defect
184 observed in *Ppa-mec-3* and *Ppa-mec-6* we also tested these mutants for kin-recognition defects. For both
185 *Ppa-mec-3* and *Ppa-mec-6* mutants, kin-recognition was robustly maintained indicating no deficiency in
186 this process (supplementary Fig. 2C). Therefore, defects in mechanosensation are specific to prey detection
187 and do not influence other predatory traits.
188

189 **Chemosensation and mechanosensation synergistically influence prey detection**

190 The partial defect in prey detection observed in the *Ppa-mec-3* and *Ppa-mec-6* mutants is similar
191 to that previously describe in cilia deficient mutants (18). Cilia are complex organelles, and in nematodes
192 they are essential for the detection of many environmental cues. In both *C. elegans* and *P. pacificus,* some
193 of the strongest cilia deficiencies are observed in mutants defective for the transcription factor, DAF-19,
194 which acts as the master regulator of ciliogenesis (18, 39, 40). Curiously, while mutations in *Cel-daf-19*
195 cause aberrant dauer entry, no abnormal dauer phenotypes result from *Ppa-daf-19* mutations in *P. pacificus,*
196 reinforcing the distinct evolutionary trajectories regulating this developmental process between these
197 species (41). Furthermore, accompanying the numerous chemosensory defects in *Ppa-daf-19*, these mutants
198 are also defective in prey detection (18). Therefore, to disentangle the roles of chemosensation and
199 mechanosensation, we assessed the *Ppa-mec-3* and *Ppa-mec-6* mutants alongside *Ppa-daf-19.* We found
200 that while *Ppa-daf-19* mutants showed chemosensory defects in their attraction to a bacterial food source
201 and in their aversion to octanol, both *Ppa-mec-3* and *Ppa-mec-6* responded as wildtype animals to these
202 cues (Fig. 3 A and B). This indicates both *Ppa-mec-3* and *Ppa-mec-6* are not defective for chemosensation.
203 In contrast, while both *Ppa-mec-3* and *Ppa-mec-6* are mechanosensory defective, the touch response of

204 *Ppa-daf-19* mutants was similar to wild type animals (supplementary Fig. 3 B-D). A similar observation
205 has also been reported in *C. elegans,* where only mild mechanosensory defects are observed in *Cel-daf-19*
206 mutants (42). Thus, mechanosensory defects appear specific to *Ppa-mec-3* and *Ppa-mec-6,* while *Ppa-daf-*
207 19 mutants are mostly associated with chemosensory defects. As both groups of mutants are defective for
208 prey detection, but neither fully abrogates the *P. pacificus* predatory abilities, we next assessed if these
209 sensory inputs act synergistically. We found that the predation defect was further exacerbated in double
210 mutants of *Ppa-mec-6; Ppa-daf-19* as well as *Ppa-mec-3; Ppa-mec-6; Ppa-daf-19* triple mutants, but
211 crucially, some killing was still maintained (Fig. 3C). Therefore, chemosensation and mechanosensation
212 act together for prey detection. Remaining killing abilities may act through some residual function in these
213 sensory pathways or through another as yet unidentified stimuli.
214

215 **Behavioural tracking and state predictions**

216 Quantifying the number of *C. elegans* corpses generated by *P. pacificus* predators provides a robust
217 assessment of overall killing ability (11). However, understanding the sensory-motor transformations
218 underpinning prey contact requires a more detailed behavioural analysis. We recently developed an
219 automated behavioural tracking and machine learning model to identify and quantify aggressive
220 behavioural states associated with predation and further analyse these complex behaviours (17, 43). Using
221 this method, the *P. pacificus* behavioural repertoire can be divided into six states. These consist of three
222 predatory associated states including 'predatory search', 'predatory biting' and 'predatory feeding' (Fig.
223 3D). Additionally, three non-predatory behaviours including a 'dwelling' state and two 'roaming' states
224 exist which are similar to behavioural states observed in *C. elegans* (15, 17). The two most predictive
225 features of predation states are velocity and pumping rate. By observing the joint distribution of these two
226 features, it is possible to visualize the prevalence of predatory and non-predatory states (Fig. 3D). We used
227 a machine learning model that was previously trained on behavioural data using both unsupervised and
228 supervised methods (17) to investigate behavioural state occupancy in our predation mutants compared to
229 wildtype animals (Fig. 3D-F , and supplementary Fig. 3E-G). In the mechanosensory defective *Ppa-mec-6*
230 and *Ppa-mec-3,* as well as the chemosensory defective *Ppa-daf-19* mutants, we found a significant increase
231 in the duration and total time spent into the 'predatory search' state. This may be indicative of a
232 compensatory mechanism whereby the loss of one sense enhances utilisation of the remaining senses. This
233 is further supported by the absence of the increased 'predatory search' state in mutants lacking both sensory
234 modalities (Fig. 3F). Instead, these *Ppa-mec-6; Ppa-daf-19* double mutants show a significant increase in
235 the non-predatory 'search' and 'roaming' states, indicating a switch away from predatory states and into
236 exploratory behaviours. This is similar to observations in *C. elegans* where the loss of one or multiple
237 sensory modalities results in modifications to the performance of the remaining senses and induces

behavioural adjustments (28). Furthermore, 'predatory biting' state occupancy was similar to wildtype animals in both *Ppa-mec-6* and *Ppa-mec-3* mutants while, in *Ppa-daf-19* this state was significantly reduced. Therefore, predatory behavioural states are modulated through signals received through the *P. pacificus* sensory systems with both chemosensory and mechanosensory modalities influencing distinct but overlapping aspects of prey detection.

Prey detection systems converge on the IL2 sensory neurons

As distinct mechanosensory and chemosensory inputs contribute to the *P. pacificus* predatory abilities, we investigated if they act through discrete independent neurons, or if instead, they converge into the same sensory pathways. To resolve this, we generated a reporter strain expressing *Ppa-mec-6p*::Venus and *Ppa-daf-19p*::RFP and identified the specific prey detection neurons involved. *Ppa-mec-6p*::Venus and *Ppa-daf-19p*::RFP co-localised and were robustly expressed in the *P. pacificus* IL2 neurons (Fig. 4A and B). These were identified based on soma position and their unique morphological features (44). Importantly, the anterior processes from this group of six neurons project into the external environment through exposed sensory endings making them strong candidates for prey detection (Fig. 4C). Additionally, we observed that *Ppa-mec-6* is co-expressed with *Ppa-mec-3* in the putative *P. pacificus* ALM and PLM body neurons as well as the FLP head neurons (supplementary Fig. 4A and B). Alongside this, *Ppa-daf-19* shows low expression in few other head neurons (Fig. 4B). As in *C. elegans,* many sensory neurons in *P. pacificus* are ciliated and this is not restricted to the IL2 sensory neurons (40). Therefore, it is somewhat surprising that the most robust *Ppa-daf-19* expression is observed in the IL2 neuron cluster. However, as there are several large introns in the *Ppa-daf-19* gene structure which contain enhancers and other epigenetic signatures (45), we predict these may contribute additional regulatory elements for further expression in other ciliated neurons. These may currently be missing from our *Ppa-daf-19p*::RFP reporter. Thus, both mechanosensory and chemosensory prey detection systems converge on the same head neurons with sensory projections exposed to the external environment, likely acting as the first point of contact with potential prey.

Functional inhibition of *Ppa-mec-6* expressing neurons disrupts mechanosensation and predation

Finally, with the convergence of sensory stimuli in the IL2 neurons and the importance of *Ppa-mec-6* for prey detection, we investigated the requirements of *Ppa-mec-6* expressing cells for predation. We expressed a histamine-gated chloride channel (HisCl) under the control of the *Ppa-mec-6* promoter. This method, recently established in *P. pacificus,* enables inducible inhibition of target neurons upon the exogenous addition of histamine as neurons become hyperpolarised (46). We first verified that the construct and treatment did not affect worm health. Developmental time was the same across wildtype and transgenic *Ppa-mec-6p*::HisCl animals, both alone and in the presence of histamine, indicating no adverse effects

272 (supplementary Fig. 4C). Furthermore, mouth form also remained at wildtype ratios indicating *Ppa-mec-6*
273 expressing cells, including the IL2 sensory neurons, do not influence this trait (supplementary Fig. 4D).
274 Next, we assessed the requirement of the *Ppa-mec-6* expressing neurons for mechanosensation and
275 chemosensation. Both body touch and nose touch response were significantly reduced upon silencing of
276 the *Ppa-mec-6* positive neurons although the effect on nose touch was much greater than the body touch
277 response (Fig. 4D, supplementary Fig. 4E and F). We also observed no defect in the response to our
278 chemosensory stimuli upon neuronal silencing (supplementary Fig. 4G and H). Finally, we tested the
279 consequences of this inhibition on predation. Both the number of corpses and prevalence of predatory states
280 were reduced when *Ppa-mec-6p*::HisCl expressing worms were treated with histamine (Fig. 4E-G and
281 supplementary Fig. 4I). Automated identification of the different behavioural states indicated that time
282 dedicated to all three predatory behaviours - search, biting and feeding were reduced. These reductions
283 were accompanied by an increase in two of the exploratory behaviours - search and roaming. Thus, neurons
284 expressing *Ppa-mec-6,* including the IL2 sensory neurons, are required for predation.
285

286 **Discussion**

287 A central aspect associated with the evolution of predatory behaviours hinges on an organism's
288 ability to detect potential prey. Fundamental to this are adaptations to sensory abilities that enable an
289 organism to perceive, process and respond to potential prey cues and direct predatory behaviours
290 appropriately. In the nematode *P. pacificus,* we have found that the evolution of predation is associated
291 with the diversification and specialisation of both mechanosensory and chemosensory modalities to also
292 encompass prey detection (Fig. 4H). This is beyond their previously described function in the model species
293 *C. elegans*. The co-option and neofunctionalisation of sensory systems are a frequently observed
294 phenomenon. For example, the lateral line system, used to detect water movements and vibrations in many
295 fish species, has evolved electroreception capabilities in sharks, rays and skates (47). Similarly, certain
296 snake species including pit vipers, pythons and some boas have evolved infra-red detection through
297 adaptations to the temperature-sensitive skin thermotransduction receptor TRPA1. This enables these
298 species to hunt warm blooded prey in near total darkness, while in other snakes it is a mechanism to regulate
299 body temperature (48). Examples of sensory co-option events are not restricted to animals and can also be
300 readily found in plants including carnivorous Venus flytrap and sundew species, whereby ancestral
301 mechanosensory channels are instead used for sensing and prey capture (49). Therefore, our findings
302 support a well-established link between sensory system evolution and behavioural diversity across a wide
303 range of taxa.

304 In *P. pacificus*, the co-option and integration of multiple sensory modalities, suggests that predation
305 is not solely dependent on enhancements and adaptations to a single sensory pathway but rather on the

306 evolution of multiple interacting systems which fine tune prey capture. In this nematode species, it is both
307 chemosensation and mechanosensation that are required for efficient predation. Similar multimodal
308 mechanisms of predation can be observed in other invertebrates, including other species which also lack
309 visual inputs or those which hunt in low light environments. These include species of octopus, which utilise
310 chemotactile receptors on their tentacles to identify potential prey through a mechanism of contact-
311 dependent aquatic chemosensation (50). Additionally, cone snails are carnivorous molluscs that hunt fish,
312 worms or other snails and utilize chemosensation to first detect the presence of chemicals secreted by their
313 prey, and subsequently use vibration sensing and mechanoreception to determine prey position. They then
314 shoot a venomous harpoon-like tooth to immediately immobilise and feed on their target (51). In *P.*
315 *pacificus*, our data shows that both chemosensation and mechanosensation are important for predation, and
316 defects in either system significantly reduce killing ability. Additionally, from our behavioural state studies
317 of these mutants, we find defects in *Ppa-daf-19* chemosensory mutants are more severe and are associated
318 with aberrations in the 'predatory biting' state, alongside increased 'predatory search' occupancy. A similar
319 'predatory search' occupancy increase is also detected in *Ppa-mec-3* and *Ppa-mec-6* mutants. We
320 hypothesize that the increased 'predatory search' state occupancy in both sensory modalities is a
321 compensatory mechanism whereby *P. pacificus* switches dependency to the unimpaired sense in an attempt
322 to maintain its predatory behaviours. This is further validated by the loss of this increase in mutants lacking
323 both the predatory-associated mechanosensory and chemosensory components. Indeed, sensory loss in *C.*
324 *elegans* has also been shown to alter the performance of remaining sensory modalities resulting in distinct
325 behaviours (28). Furthermore, while the mechanosensory *Ppa-mec-6* and *Ppa-mec-3* as well as
326 chemosensory *Ppa-daf-19* mutants show reduced killing abilities, *Ppa-mec-6* and *Ppa-mec-3* mutants were
327 found to occupy 'predatory biting' states similar to wildtype, while this state was reduced in *Ppa-daf-19*.
328 Therefore, both sensory inputs likely have specific functions during predation, such that chemosensation is
329 potentially required throughout these behaviours while mechanosensory systems may be associated with
330 the initial steps of the predator-prey contact.

331 Both *daf-19* and *mec*-3 are transcription factors and influence genes associated mostly with
332 chemosensation and mechanosensation respectively (20, 40). This makes it difficult to disentangle the
333 precise molecular mechanisms associated with the emergence of the predatory behaviour in *P. pacificus*
334 using these mutants alone. However, by focusing on the role of mechanosensation, we have been able to
335 identify *Ppa-mec-6* as a specific molecular component that has acquired additional functions in *P. pacificus*
336 associated with its predatory feeding. In *C. elegans*, *Cel-mec-6* is a known to interact with several
337 DEG/EnAC type subunits with the best characterised being *Cel-mec-4* and *Cel-mec-10* which form a
338 mechanosensory ion channel responsible for the gentle touch response (24, 29, 52). Within this complex
339 *Cel-mec-6* is a small auxiliary protein that is not a pore-forming subunit itself, but is necessary for proper

340 channel function. In *P. pacificus,* we find mutations in any of *Ppa-mec-4, Ppa-mec-10* or *Ppa-mec-6* result
341 in mechanosensory defects, but it is only *Ppa-mec-6* that has additional predation-specific abnormalities.
342 Thus, while *Ppa-mec-6* may interact with *Ppa-mec-4* and *Ppa-mec-10* to regulate mechanosensation as in
343 *C. elegans*, it is also likely involved with other as yet unknown components and may form a distinct
344 mechanosensory channel involved in prey detection. These components require further identification.
345 By analysing the localization of *Ppa-mec-6*, we observed robust expression in the six head sensory
346 IL2 neurons where it is also expressed in *C. elegans* (21) . These neurons are easily identified in *P. pacificus*
347 by their morphology and soma location, which also show a distinct placement compared to *C. elegans* (44,
348 53). In both species, the IL2 neurons project neurites toward the nematode nose with the sensory endings
349 exposed to the external environment. In *C. elegans,* these neurons regulate dauer formation and nictation
350 behaviours, and are thought to be both chemosensory and mechanosensory (54, 55). Furthermore, they
351 release extracellular vesicles potentially involved in communication (56, 57). In *P. pacificus,* our results
352 show that IL2 inhibition also prevents the acquisition of sensory information necessary for prey detection.
353 Crucially, recent studies in *P. pacificus* identified the IL2 neurons as regulators of predatory feeding states
354 which depend on the balancing actions of octopamine and tyramine (17). Octopamine induces predatory
355 states while tyramine initiates more docile bouts and IL2 neurons express octopamine receptors necessary
356 for the predatory states in *P. pacificus*. Accordingly, our findings that these neurons express *Ppa-mec-6* as
357 well as *Ppa-daf-19* reinforces their importance as prime candidates for detecting and determining prey
358 contact events. Moreover, the convergence of both mechanosensory and chemosensory inputs, as well as
359 behavioural state modulatory mechanisms, in the *P. pacificus* IL2 neurons demonstrates that even relatively
360 simple circuits can be remodelled to accommodate complex and dynamic behaviours including predation.
361 Therefore, taken together, our findings provide new insights into how sensory systems are co-opted and
362 refined to generate behavioural diversity, and demonstrate the importance of sensory perception and
363 evolutionary adaptations for establishing novel behavioural traits.
364

365 ## Materials and methods

366 ### Worm maintenance

367 *P. pacificus* (PS312 and derived strains) or *C. elegans* (N2), were maintained on nematodes growth
368 media (NGM) 6 cm plates seeded with 300 µl *Escherichia coli* (OP50) at 20ºC. All *P. pacificus* strains used
369 are listed in supplementary table 1A. The *C. elegans* N2 strain was provided by the CGC, which is funded
370 by NIH Office of Research Infrastructure Programs (P40 OD010440).
371

372 ### Orthologue identification

373 We generated a mechanotransduction channel list from wormbook (22) and obtained published
374 genome assemblies for eight nematode species belonging to different clades identified by Blaxter et al (23).
375 These species include: *Pristionchus pacificus* (10), *Caenorhabditis elegans* (release WS271, 2019,
376 WormBase website (58)), *Strongyloides ratti* (59), *Bursaphelenchus xylophilus* (60), *Brugia malayi* (61,
377 62), *Ascaris suum* (63), *Romanomermis culicivorax* (64) and *Trichinella spiralis* (65). When multiple
378 annotated isoforms were available, only one was considered for analysis. Orthologous were determined
379 using OrthoFinder (66).
380

381 **Generation of new strains**

382 Mutations were induced by CRISPR/Cas9 (IDT) by co-injection of the sgRNA for the gene of
383 interest while using a sgRNA targeting *Ppa-prl-1* as a marker as previously described (67). sgRNAs were
384 made by mixing crRNA (IDT) and tracrRNA (IDT) in equal volume and quantity and incubated for 5 min
385 at 95ºC. After letting them cooldown 5 min at room temperature, up to three sgRNA were mixed with the
386 Cas9 and 5 min later Tris-EDTA (TE, Promega) was supplemented to reach the concentration of 18.1 µM
387 for sgRNA and 12.5 µM for Cas9. This mix was centrifuged for 10 min at maximum speed at 4ºC. The
388 resulting mix was used to inject *P. pacificus* adults in the gonads area (Axiovert 200, zeiss and Eppendorf
389 set up). P0 injected worms were singled out and laid eggs overnight. Once the progeny had developed
390 enough, plates were screened for a roller phenotype induced by the dominant mutation in *Ppa-prl-1* pointing
391 to successful injection. Around 50 worms were genotype from identified plates for the gene of interest using
392 PCR (Qiagen) followed by sanger sequencing (Eurofins). The sgRNA and primer sequences used as well
393 as the wild-type sequences and generated mutation are provided in supplementary table 1B. Two guide
394 RNA were used for *Ppa-mec-3* to target both isoforms. All mutations generated are predicted to lead to an
395 early stop codon or frameshift with the exception of one allele of *Ppa-mec-3 (bnn61)* and one allele of *Ppa-*
396 *trp-2 (bnn51*) presented in supplementary figures. Mutations were generated in the *P. pacificus* PS312
397 strain.

398 Behavioural tracking and state predictions required an integrated *Ppa-myo-2p*::RFP (17). In
399 addition, mouth morph ratio is influenced by *Ppa-daf-19* which results in a strong st bias unsuitable for
400 predation assays (18). Therefore, predatory morphs eu were induced alongside *Ppa-daf-19* through
401 generation of additional mutations in *Ppa-nag-1; Ppa-nag-2* (18) in the *Ppa-myo-2p*::RFP background.
402 Accordingly, this strain JWL118 has a 100% Eu mouth morphs (Supplementary Fig. 3A). For experiments
403 involving *Ppa-daf-19*, all comparative experimental strains also carry *Ppa-nag-1; Ppa-nag-2* mutations
404 based on the control strain JWL147 (see supplementary table 1).
405

406 **Generation of reporter lines**

407 TurboRFP and GFP sequences optimized for *P. pacificus* were retrieved from plasmid pZH009 and
408 pZH008 respectively (9). A Venus reporter was optimised for *P. pacificus* as previously described (9).
409 Promotor sequences consisted of the indicated number of nucleotides preceding the ATG according to *P.*
410 *pacificus* genome (10): *Ppa-mec-6* (949 bp), *Ppa-mec-3* (932 bp), *Ppa-daf-19* (719 bp) promotor sequences.
411 *Ppa-daf-19p*::RFP (pMR027, Genscript) and *Ppa-mec-6p*::Venus (pMR022, eurofins) were made by gene
412 synthesis and *Ppa-mec-3p*::RFP (pMR005) by cloning. For generating stable transgenic lines, animals were
413 injected with a mix containing 60 ng/µl purified gDNA (NEB Monarch purification kit) along with 5- 10
414 ng/µl plasmid of interest all digested with HindIII. Prior to each injection, the mix was centrifuged at
415 maximum speed at 4ºC for 10 min. Injection were made in *P. pacificus* adult gonads (Axiovert 200, zeiss,
416 and Eppendorf set up). Progeny worms carrying the construct of interest were identified using the epi-
417 fluorescence microscope (Axio Zoom V16; Zeiss). Confocal images were acquired using a stellaris
418 microscope (Leica) with a 63x objective at water immersion.
419

420 **Chemosensory assays**

421 Attraction toward OP50 was tested using previously developed assays with minor modifications
422 (40). 20 µl of an OP50 overnight culture was pipetted onto a 6 cm unseeded plate 1.5 cm from the edge and
423 left at room temperature overnight. Plates where then kept in the fridge until use. 50 adult worms from
424 plates almost depleted of food were placed at the opposite side of the bacterial lawn at around 1.5 cm of the
425 border making sure to not transfer any bacteria when doing so. After 8 hours the number of worms at the
426 bacterial lawn and the total number of worms still alive in the plates were determined. Plates were scored
427 if they had at least 30 worms left at the end of the assay.
428 To assess worm behaviour toward 1-octanol, we adapted existing protocols (41). Adult worms were
429 washed off with M9 and left on an unseeded plate for 3 hours to remove bacteria. Prior to starting the assay,
430 two drop of 1.2 µl of sodium azide 1M was deposit 3 cm apart on opposite side of a 6 cm unseeded plate.
431 100 worms were placed in the middle line between the two drops and immediately 1µL of 100% ethanol
432 was put as control on top of one of the sodium azide deposits and 1 µl of 100% 1-octanol (sigma-aldrich)
433 over the other. The assay plates were left for 16 hours at 20°C before assessing worm position. Only worms
434 within a 2 cm radius of the drop up to the midline were taking into account leading to a total of at least 40
435 worms. Chemosensation index was calculated as the ratio between the number of worm closer to the 1-
436 octanol minus those closer to the ethanol relative to the total number of worms. For both assays 10 replica
437 were made over at least three different days.
438

439 **Touch assays**

440 Touch assays were performed as described for *C. elegans* with minor modifications (22). Worms
441 were transferred to unseeded plates and left to recover for several minutes prior to being utilised in one of
442 the three assays. Harsh touch assays consisted of touching the worm between its vulva and its tails with the
443 platinum pick used in every day worm maintenance. For the gentle touch assays, the worm was caressed
444 with an eyelash (taped to a wood skewer pick for handling) between its vulva and its tails. For both assays,
445 each worm was tested ten times and the number of times that trigger a reaction was assessed. Due to the
446 fact that some of our strains appear lethargic we did not only consider forward movement as a reaction but
447 any change in worm state occurring upon contact. To assess sensation of the nose, the eyelash was presented
448 to the nose of the worm ten time and again all sign of detection were considered (backward movement or
449 head bending). At least 30 worms over at least 3 different days were assessed for each test and strain.
450

451 **Corpse assay**

452 Predatory behaviour was tested as previously described with modifications (11, 17). *C. elegans*
453 larvae were collected from plates depleted in food just after hatching using M9 and passed through 20 µm
454 filter to remove the other developmental stages. After centrifugation (2000 rpm, 1 min), ~1 µl of larvae was
455 put off centre of a 6 cm unseeded plate, see supplementary figure 1A. In parallel, predators consisting of
456 young adult *P. pacificus* of the strain of interest were picked onto another unseeded plates. Both predators
457 and prey were left for 2 hours to allow the larval prey to spread and predator to starve. 5 predators were
458 added on the plates and a copper arena 2.25 cm^2 was put around them. Assays were left for 2 hours then
459 two pictures of the arena were taken at ~20x (each field covered a quarter of the arena) at least 10 second
460 apart (Axio Zoom V16; Zeiss). The two images were process with Fiji using the 'max' set up and corpses
461 were manually count on the resulting image. To assess kin recognition PS312 *P. pacificus* larvae were used
462 as prey with 20 predator and the assay took place without the arena for 24 hours. Corpses were counted
463 under the bench microscope (stemi 508, zeiss). For both assay 10 replicates were conducted at least three
464 different days. To increase the power of our assay and detect smaller variation between strain, 20 replicas
465 were made for figure 3.
466

467 **Mouth form assessment**

468 Worms were grown in OP50 plates until a high number of adults was reach. Worms were then
469 washed in M9 and placed on a slide containing sodium azide to immobilized them. The number of eu and
470 st worms were counted under an Axiovert 200 (zeiss) at 10x or 20x. Mouth form was controlled from 5
471 different plates over at least three different days with a minimum of 30 animals scored per assay.
472

473 **Feeding assay with PharaGlow**

474 PharaGlow experiments were performed as described previously (17). Briefly, adult worms with a
475 fluorescent pharynx marker (*Ppa-myo-2*p::RFP) were picked onto an unseeded plates and left for a 2 hour
476 starvation period. 30 worms were picked onto unseeded assay plates containing *C. elegans* larvae made as
477 for the killing assays (see above) but with twice the density to saturate the plate in larvae. To maintain the
478 worms inside the field of view, a copper arena 2.25 cm^2 was put around the assay animals. Worms were
479 acclimated to their new environment for 15 min before recording. Recording was made with an epi-
480 fluorescence microscope (Axio Zoom V16, Zeiss) at 1x effective magnification (60 N-C ⅔'' 0.5 x, Zeiss)
481 and Basler camera (acA3088-57um, BASLER). Light intensity was set at 100% and acquisition time was
482 adjusted to use the full range of intensity without saturating the signal. Images were acquired at 30 Hz for
483 10 min. Images were then compressed and processed with the python package PharaGlow
484 (https://github.com/scholz-lab/PharaGlow), (43) adapted for *P. pacificus* (17) with the following
485 parameters (subtract:1, smooth:3, dilate:3, tfactor:0.9, thresholdWindow:50, bgWindow:500, length:70,
486 watershed:100, minSize:250, maxSize:1000, searchRange:10, memory:30, minimalDuration:1800,
487 widthStraight:10, pad:5, nPts:50, linewidth:2). The quality of extracted movies was manually assessed and
488 any worms with no sign of activity throughout the recording length were considered dead or damaged and
489 removed from the analysis. Post-processing to calculate the velocity and pumping rate was done using a
490 previously developed python script and finally automatic behavioural prediction were assigned using the
491 git-hub package PpaPred as described previously (https://github.com/scholz-lab/PpaPred), (17). Worms
492 were recorded over at least three different days.
493

494 **Inhibition of neurons by histamine chloride channels**

495 The *Ppa-mec-6* promotor from our reporter construct *Ppa-mec-6p*::Venus (pMR022) was cloned
496 in front of the *P. pacificus* codon optimized histamine chloride channel from plasmid pLJ149 (17) forming
497 plasmid pLB010. Transgenic line JWL237 carrying both pMR022 and pLB010 was generated as described
498 above in the wildtype PS312 background. JWL237 was then crossed in the *Ppa-myo-2p*::RFP background
499 (JWL27) for tracking experiments. Only worms displaying green fluorescent were used for experiments.
500 Histamine plates were made by the addition of histamine chloride to the NGM before pouring to
501 reach a final concentration of 10 mM. Plates were kept and used in the dark to preserve the histamine.
502 Touch, chemosensation and feeding assays were made as described above with worm transferred to the
503 histamine plates at least 10 minutes before performing the assay or from the starvation period when
504 applicable. For corpses assays, copper arenas were not used as they reacted with the histamine chloride and
505 due to the wide field of exploration, images could not be taken and instead corpses were counted manually
506 after 2 h exposure to predators. For developmental assay and mouth form assessment, histamine plates were

507 seeded as usual with 300 µl of OP50 and around 100 J2 larvae were added following filtration (20 µm filter,
508 Millipore). After 4 days at 20ºC, the number of eu or st animals were assessed.
509

510 **Data representation and statistical analysis**

511 Box plot illustrates data distribution with quartiles Q1, Q2, and Q3 representing the 25th, 50th,
512 and 75th percentiles, respectively. The box, bounded by Q1 and Q3, includes a thicker line at the median
513 (Q2). Whiskers show the range where most values fall. Analysis of chemosensory assay, touch assay,
514 corpses assays and mouth form ratio was made with R software and its package prettyR with significance
515 determine using one-direction Wilcoxon Mann Whitney with Benjamini-Hochberg correction (68).
516 Analysis of the state prediction results (relative time in state, mean bout duration, transition rates) were
517 done with python as describe previously (17) relying on Wilcoxon Mann Whitney with Bonferroni
518 correction. In figures, statistics results are display as follow: non-significant (ns), p-value ≤ 0.05 (*), ≤ 0.01
519 (**), ≤ 0.001 (***), ≤ 0.0001 (****).
520

521 **Acknowledgments**

522 We would like to thank all the Lightfoot and Scholz labs for useful discussions, Desiree Goetting
523 for critical reading of the manuscript, Wolfgang Bönigk for plasmid cloning (Genetics Facility, MPI for
524 Neurobiology of Behavior-caesar), the Imaging facility for assistance (MPI for Neurobiology of Behavior-
525 caesar) and Jürgen Berger for SEM imaging presented in figure 5 (MPI for Biology). The strains PS312
526 and RS3238 were provided by the Sommer lab (MPI for Biology, Tübingen).
527
528

529 **Figure legends**

530 **Figure 1 *Ppa-mec-3* regulates touch avoidance and prey detection.**

531 (A) A *P. pacificus* adult predator (right) attacks a *C. elegans* larvae (left). Scale bar is 100 µm. (B)
532 Representative image of a *P. pacificus* adult expressing *Ppa-mec-3p*::RFP (top, magenta). Putative *P.*
533 *pacificus* neuronal identity is based on *C. elegans* soma placement and known mechanosensory function.
534 Scale bar is 100µm. (C) Mechanosensory assays to harsh touch, (D) gentle touch, and (E) nose touch. Each
535 assessment is the result of ten consecutive trials of each worm. At least 30 worms were tested per strain.
536 (F) Number of *C. elegans* corpses counted after two hours of contact with the indicated *P. pacificus* strains
537 as predator. At least 10 assays were performed. Statistical tests: one-direction Wilcoxon Mann Whitney
538 with Benjamini-Hochberg correction, non-significant (ns), p-value ≤ 0.05 (*), ≤ 0.01 (**), ≤ 0.001 (***), ≤
539 0.0001 (****). Schematics were made with biorender.

540

541 **Figure 2 Mechanosensation is required for efficient predation.**

542 (A) Table analysing the number of mechanosensory gene paralogues compared to *C. elegans*. Species of
543 free-living nematodes (brown), plant parasite nematodes (green) and animal parasite nematodes (black) are
544 compared. Their evolutionary tree is presented on the left with the nematode clade marked. (B)
545 Mechanosensory assays to harsh touch, (C) gentle touch, and (D) nose touch for *P. pacificus* mutants in
546 putative mechanosensory genes. Each assessment is the result of ten consecutive trials of each worm. At
547 least 30 worms were tested per strain. (E) Number of *C. elegans* corpses counted after two hours of contact
548 with the indicated *P. pacificus* putative mechanosensory mutants as predators. At least 10 assays were
549 performed per mutant. Statistical tests: one direction Wilcoxon Mann Whitney with Benjamini-Hochberg
550 correction, non-significant (ns), p-value ≤ 0.05 (*), ≤ 0.01 (**), ≤ 0.001 (***), ≤ 0.0001 (****). Schematics
551 were made with biorender.

552

553 **Figure 3: Chemosensation and mechanosensation synergically influence prey detection.**

554 (A) Chemotaxis index analysing the aversive response of *Ppa-mec-3, Ppa-mec-6* and *Ppa-daf-19* to 1-
555 octanol. Each genotype was assessed 10 time. (B) Percentage of *Ppa-mec-3, Ppa-mec-6* and *Ppa-daf-19*
556 mutants finding a bacterial OP50 food source after 8 hours. Each genotype was assessed 10 times.
557 (C) Number of *C. elegans* corpses generated after two hours of exposure to the indicated *P. pacificus*
558 mutants as predator. At least 20 assays were performed. (D) Schematic of behavioural tracking and machine
559 learning workflow to track feeding behaviour and determine behavioural states based on a *Ppa-myo-2*::RFP
560 pharyngeal fluorescence marker (established in Eren et al 2024). (E) Joint probability density map of
561 velocity (µm/s) and pumping rate (Hz) for animals corresponding to the genotypes *Ppa-mec-6, Ppa-daf-19,*
562 and *Ppa-mec-6; Ppa-daf-19.* The number of worms is indicated in the top right corner. (F) Time spent in
563 each behavioural state normalised to the total track duration. Statistical tests: Significance from comparison
564 to wild-type (black) and to *daf-19* single mutant (green) was assessed using one direction Wilcoxon Mann
565 Whitney with Benjamini-Hochberg correction (A-C), Mann-Whitney U-test with a Bonferroni correction
566 (F). non-significant (ns), p-value ≤ 0.05 (*), ≤ 0.01 (**), ≤ 0.001 (***), ≤ 0.0001 (****). Schematics were
567 made with biorender. Predatory (Pr.)

568

569 **Figure 4: Predation is disrupted by inhibition of *Ppa-mec-6* expressing cells**

570 (A) Head of a worm expressing *mec-6p*::Venus (top, green) and *daf-19p*::RFP (middle, magenta). Co-
571 expression of both *Ppa-mec-6* and *Ppa-daf-19* visible in the merge image. IL2 neurons are indicated. Scale
572 bar is 100 µm. (B) Representative image of a worms expressing *Ppa-mec-6p*::Venus (top, green) and *Ppa-*
573 *daf-19p*::RFP (middle, magenta) and the merge (bottom). Scale bar is 100 µm. (C) Scanning electron

574 microscopy image of the anterior of a *P. pacificus* adult. The *P. pacificus* mouth opening is surrounded by
575 protrusions of the 6 inner labial IL2 sensilla neurons (arrow). Scale bar is 3 µm (D) Mechanosensory assays
576 of nose touch for *P. pacificus* worms for each condition: wild-type worms treated with histamine and worms
577 expressing HisCl channel under the control of *Ppa-mec-6* promotor in absence (-) or presence (+) of
578 histamine. Each datapoint is the result of ten consecutive trials on an individual worm. At least 30 worms
579 were tested per condition. (E) Number of *C. elegans* corpses generated after two hours of exposure to the
580 indicated *P. pacificus* worms as predator in absence (-) or presence (+) of histamine. 20 assays were
581 performed. (F) Joint probability density map of velocity (µm/s) and pumping rate (Hz) for animals
582 corresponding to condition described in (D). The number of worms is indicated in the top right corner. (G)
583 Time spent in each behavioural state normalised to the total track duration. (H) Putative model of the
584 evolutionary diverse role for mechanosensation between *C. elegans* and *P. pacificus*. In both species,
585 mechanosensation triggers an avoidance response which rely on *mec-3, mec-6, mec-4* and *mec-10.* In
586 addition, in *P. pacificus,* contact can trigger predatory behaviour when the IL2 perceive mechanical or
587 chemical stimuli. The perception of the predatory specific mechanical stimuli, acts through the
588 mechanosensory pathway components *Ppa-mec-3* and *Ppa-mec-6.* Statistical tests: Significance from
589 comparison to wild-type (black) and to *Ppa-mec-6p*::HisCl untreated worms (brown) was assessed using
590 one direction Wilcoxon Mann Whitney with Benjamini-Hochberg correction(D-E), Mann-Whitney U-test
591 with a Bonferroni correction (G). non-significant (ns), p-value ≤ 0.05 (*), ≤ 0.01 (**), ≤ 0.001 (***), ≤
592 0.0001 (****). Predatory (Pr.) Schematic was made with biorender.
593
594 **Supplementary Figure 1: Mechanosensation and predation in *P. pacificus***
595 (A) Schematic of the corpse assay protocol. Five starved *P. pacificus* predators of the strain of interest are
596 introduce in an area with an abundancy of *C. elegans* larvae. After 2 h, predatory success is assessed by
597 counting the number of larval corpses inside the arena. In the image corpses can be observed inside the
598 circles. Scale bar is 500 µm. (B) Mechanosensory assays to harsh touch, (C) gentle touch, and (D) nose
599 touch. Each assessment is the result of ten consecutive trials of each worm. At least 30 worms were tested
600 per strain. (E) Number of *C. elegans* corpses counted after two hours of contact with the indicated *P.*
601 *pacificus* strains as predator. At least 10 assays were performed. Statistical tests: one direction Wilcoxon
602 Mann Whitney with Benjamini-Hochberg correction, non-significant (ns), p-value ≤ 0.05 (*), ≤ 0.01 (**),
603 ≤ 0.001 (***), ≤ 0.0001 (****). Schematics were made with biorender.
604
605 **Supplementary Figure 2: Mechanosensation does not affect developmental plasticity or kin-**
606 **recognition**

607 (A) *P. pacificus* is developmentally plastic leading to one of two mouth forms, stenotomatous mouth (st,
608 bottom) with the dorsal tooth (blue) or eurytomatous (eu, top) with an additional subventral tooth (red) and
609 a wider opening. Scale bar is 10 µm. (B) Percentage of eu was assess 5 time for each strain. (C) Number of
610 wild-type *P. pacificus* corpses counted after 24 hours of contact with the indicated *P. pacificus* strains as
611 predator. Statistical tests: one direction Wilcoxon Mann Whitney with Benjamini-Hochberg correction,
612 non-significant (ns), p-value ≤ 0.05 (*), ≤ 0.01 (**), ≤ 0.001 (***), ≤ 0.0001 (****). Schematics were made
613 with biorender.
614

615 **Supplementary Figure 3: Behavioural analysis of sensory deficient worms**

616 (A) Percentage of eu morphs were assessed 5 time for each strain. As shown in Moreno et al 2019, mutations
617 in *Ppa-daf-19* lead to a higher occurrence of st mouth form which is overcome by including mutations in
618 *Ppa-nag-1* and *Ppa-nag-2*. *daf-19** is the only time mutation of *Ppa-daf*-19 is not studied in a strain also
619 mutated for *Ppa-nag-1* and *Ppa-nag-2.* (B) Mechanosensory assays to harsh touch, (C) gentle touch, and
620 (D) nose touch. Each assessment is the result of ten consecutive trials of each worm. At least 30 worms
621 were tested per strain. (E) Joint probability density map of velocity (µm/s) and pumping rate (Hz) for
622 animals corresponding to the indicated genotypes. The number of worms is indicated in the top right corner.
623 (F) Time spent in each behavioural state normalized to the total track duration. (G) Mean duration of each
624 behaviour in B. Statistical tests: Significance from comparison to wild-type (black) and to *daf-19* single
625 mutant (green) was assessed using one direction Wilcoxon Mann Whitney with Benjamini-Hochberg
626 correction(A-D), Mann-Whitney U-test with a Bonferroni correction (F-G). non-significant (ns), p-value
627 ≤ 0.05 (*), ≤ 0.01 (**), ≤ 0.001 (***), ≤ 0.0001 (****). Schematics were made with biorender. Predatory
628 (Pr.)

629 **Supplementary Figure 5: touch neurons in *P. pacificus***

630 (A) Head of a worm expressing *mec-6p*::Venus (top, green) and *mec-3p*::RFP (middle, magenta). Co-
631 expression in the FLP of both *Ppa-mec-6* and *Ppa-mec-3* is visible in the merge image (bottom). IL2
632 neurons are indicated. Scale bar is 100 µm. (B) Representative image of a worms expressing *Ppa-mec-*
633 *6p*::Venus (top, green) and *Ppa-mec-3p*:: RFP (middle, magenta) and the merge (bottom). Putative *P.*
634 *pacificus* neuronal identity, based on *C. elegans* soma placement and known mechanosensory function, is
635 indicated in white for co-expression. Scale bar is 100 µm. (C) Percentage of worms reaching adulthood
636 after 4 days was assessed 5 time for each condition: wild-type worms and worms expressing histamine
637 chloride channel under the control of *Ppa-mec-6* promotor in absence (-) or presence (+) of histamine. (D)
638 Percentage of eu mouth form animals was assessed 5 time for each condition. (E) Mechanosensory assays
639 to harsh touch and (F) gentle touch for worms of each condition. Each data point is the result of ten
640 consecutive trials for a single worm. At least 30 worms were tested per condition. (G) Chemotaxis index

641 analysing the aversive response to 1-octanol. Each condition was tested 10 time. (H) Percentage of worms
642 finding a bacterial OP50 food source after 8 hours. Each condition was tested 10 time. (I) Mean duration
643 of each behavioural state. Statistical tests: Significance from comparison to wild-type (black) and to *Ppa-*
644 *mec-6p*::HisCl untreated worms (brown) was assessed using one direction Wilcoxon Mann Whitney with
645 Benjamini-Hochberg correction(C-H), Mann-Whitney U-test with a Bonferroni correction (I). non-
646 significant (ns), p-value ≤ 0.05 (*), ≤ 0.01 (**), ≤ 0.001 (***), ≤ 0.0001 (****). Predatory (Pr.) Schematic
647 was made with biorender.
648
649

650 # Reference:

651 1. P. Oteiza, M. W. Baldwin, Evolution of sensory systems. *Current Opinion in Neurobiology* **71**, 52–59
652 (2021).

653 2. T. O. Auer, *et al.*, Olfactory receptor and circuit evolution promote host specialization. *Nature* **579**,
654 402–408 (2020).

655 3. C. S. McBride, *et al.*, Evolution of mosquito preference for humans linked to an odorant receptor.
656 *Nature* **515**, 222–227 (2014).

657 4. A. Wada-Katsumata, J. Silverman, C. Schal, Changes in taste neurons support the emergence of an
658 adaptive behavior in cockroaches. *Science* **340**, 972–975 (2013).

659 5. H. Jiao, *et al.*, Loss of sweet taste despite the conservation of sweet receptor genes in insectivorous
660 bats. *Proc Natl Acad Sci U S A* **118**, e2021516118 (2021).

661 6. Y. Toda, *et al.*, Early origin of sweet perception in the songbird radiation. *Science* **373**, 226–231
662 (2021).

663 7. Z. Musilova, *et al.*, Vision using multiple distinct rod opsins in deep-sea fishes. *Science* **364**, 588–592
664 (2019).

665 8. G. G. Eren, M. Roca, Z. Han, J. W. Lightfoot, Genomic integration of transgenes using UV irradiation
666 in Pristionchus pacificus. *MicroPubl Biol* **2022** (2022).

667 9. Z. Han, *et al.*, Improving Transgenesis Efficiency and CRISPR-Associated Tools Through Codon
668 Optimization and Native Intron Addition in Pristionchus Nematodes. *Genetics* **216**, 947–956
669 (2020).

670 10. C. Rödelsperger, *et al.*, Single-Molecule Sequencing Reveals the Chromosome-Scale Genomic
671 Architecture of the Nematode Model Organism Pristionchus pacificus. *Cell Rep* **21**, 834–844
672 (2017).

673 11. M. Wilecki, J. W. Lightfoot, V. Susoy, R. J. Sommer, Predatory feeding behaviour in Pristionchus
674 nematodes is dependent on phenotypic plasticity and induced by serotonin. *J Exp Biol* **218**, 1306–
675 1313 (2015).

676 12. J. W. Lightfoot, *et al.*, Small peptide-mediated self-recognition prevents cannibalism in predatory
677 nematodes. *Science* **364**, 86–89 (2019).

678 13. J. W. Lightfoot, *et al.*, Sex or cannibalism: Polyphenism and kin recognition control social action
679 strategies in nematodes. *Sci Adv* **7**, eabg8042 (2021).

680 14. Y. Tanimoto, *et al.*, In actio optophysiological analyses reveal functional diversification of
681 dopaminergic neurons in the nematode C. elegans. *Sci Rep* **6**, 26297 (2016).

682 15. N. Zjacic, M. Scholz, The role of food odor in invertebrate foraging. *Genes Brain Behav* **21**, e12793
683 (2022).

684 16. R. L. Hong, H. Witte, R. J. Sommer, Natural variation in Pristionchus pacificus insect pheromone
685 attraction involves the protein kinase EGL-4. *Proceedings of the National Academy of Sciences*
686 **105**, 7779–7784 (2008).

687 17. G. G. Eren, *et al.*, Predatory aggression evolved through adaptations to noradrenergic circuits.
688 [Preprint] (2024). Available at: https://www.biorxiv.org/content/10.1101/2024.08.02.606321v1
689 [Accessed 17 September 2024].

690 18. E. Moreno, J. W. Lightfoot, M. Lenuzzi, R. J. Sommer, Cilia drive developmental plasticity and are
691 essential for efficient prey detection in predatory nematodes. *Proc Biol Sci* **286**, 20191089 (2019).

692 19. M. Okumura, M. Wilecki, R. J. Sommer, Serotonin Drives Predatory Feeding Behavior via
693 Synchronous Feeding Rhythms in the Nematode Pristionchus pacificus. *G3 (Bethesda)* **7**, 3745–
694 3755 (2017).

695 20. J. C. Way, M. Chalfie, mec-3, a homeobox-containing gene that specifies differentiation of the touch
696 receptor neurons in C. elegans. *Cell* **54**, 5–16 (1988).

697 21. D. Liska, Z. Wolfe, A. Norris, VISTA: visualizing the spatial transcriptome of the C.elegans nervous
698 system. *Bioinform Adv* **3**, vbad127 (2023).

699 22. M. Goodman, Mechanosensation. *WormBook* (2006). https://doi.org/10.1895/wormbook.1.62.1.

700 23. M. L. Blaxter, *et al.*, A molecular evolutionary framework for the phylum Nematoda. *Nature* **392**,
701 71–75 (1998).

702 24. Y. Chen, *et al.*, Caenorhabditis elegans paraoxonase-like proteins control the functional expression
703 of DEG/ENaC mechanosensory proteins. *Mol Biol Cell* **27**, 1272–1285 (2016).

704 25. J. R. M. Millet, L. O. Romero, J. Lee, B. Bell, V. Vásquez, C. elegans PEZO-1 is a mechanosensitive ion
705 channel involved in food sensation. *J Gen Physiol* **154**, e202112960 (2022).

706 26. S. L. Geffeney, *et al.*, DEG/ENaC but Not TRP Channels Are the Major Mechanoelectrical
707 Transduction Channels in a C. elegans Nociceptor. *Neuron* **71**, 845–857 (2011).

708 27. P. Baskaran, *et al.*, Ancient gene duplications have shaped developmental stage-specific expression
709 in Pristionchus pacificus. *BMC Evol Biol* **15**, 185 (2015).

710 28. M. Staum, *et al.*, Behavioral adjustment of C. elegans to mechanosensory loss requires intact
711 mechanosensory neurons. *PLOS Biology* **22**, e3002729 (2024).

712 29. D. S. Chelur, *et al.*, The mechanosensory protein MEC-6 is a subunit of the C. elegans touch-cell
713 degenerin channel. *Nature* **420**, 669–673 (2002).

714 30. M. Chatzigeorgiou, *et al.*, Specific roles for DEG/ENaC and TRP channels in touch and
715 thermosensation in C. elegans nociceptors. *Nat Neurosci* **13**, 861–868 (2010).

716 31. L. Han, *et al.*, Two novel DEG/ENaC channel subunits expressed in glia are needed for nose-touch
717 sensitivity in Caenorhabditis elegans. *J Neurosci* **33**, 936–949 (2013).

718 32. J. L. Rhoades, *et al.*, ASICs Mediate Food Responses in an Enteric Serotonergic Neuron that Controls
719 Foraging Behaviors. *Cell* **176**, 85-97.e14 (2019).

720 33. L. Tao, *et al.*, Parallel Processing of Two Mechanosensory Modalities by a Single Neuron in
721 C. elegans. *Dev Cell* **51**, 617-631.e3 (2019).

722 34. K. S. Kindt, *et al.*, Caenorhabditis elegans TRPA-1 functions in mechanosensation. *Nat Neurosci* **10**,
723 568–577 (2007).

724 35. R. Xiao, X. Z. S. Xu, Function and regulation of TRP family channels in C. elegans. *Pflugers Archiv :*
725 *European journal of physiology* **458**, 851 (2009).

726 36. A. C. Hart, S. Sims, J. M. Kaplan, Synaptic code for sensory modalities revealed by C. elegans GLR-1
727 glutamate receptor. *Nature* **378**, 82–85 (1995).

728 37. E. J. Ragsdale, M. R. Müller, C. Rödelsperger, R. J. Sommer, A developmental switch coupled to the
729 evolution of plasticity acts through a sulfatase. *Cell* **155**, 922–933 (2013).

730 38. M. S. Werner, *et al.*, Environmental influence on Pristionchus pacificus mouth form through
731 different culture methods. *Sci Rep* **7**, 7207 (2017).

732 39. E. A. De Stasio, *et al.*, An Expanded Role for the RFX Transcription Factor DAF-19, with Dual
733 Functions in Ciliated and Nonciliated Neurons. *Genetics* **208**, 1083–1097 (2018).

734 40. E. Moreno, *et al.*, DAF-19/RFX controls ciliogenesis and influences oxygen-induced social behaviors
735 in Pristionchus pacificus. *Evol Dev* **20**, 233–243 (2018).

736 41. W.-S. Lo, *et al.*, Evolution and Diversity of TGF-β Pathways are Linked with Novel Developmental and
737 Behavioral Traits. *Mol Biol Evol* **39**, msac252 (2022).

42. L. A. Perkins, E. M. Hedgecock, J. N. Thomson, J. G. Culotti, Mutant sensory cilia in the nematode *Caenorhabditis elegans*. *Developmental Biology* **117**, 456–487 (1986).

43. E. Bonnard, J. Liu, N. Zjacic, L. Alvarez, M. Scholz, Automatically tracking feeding behavior in populations of foraging C. elegans. *Elife* **11**, e77252 (2022).

44. S. J. Cook, *et al.*, Comparative connectomics of two distantly related nematode species reveals patterns of nervous system evolution. [Preprint] (2024). Available at: https://www.biorxiv.org/content/10.1101/2024.06.13.598904v1 [Accessed 19 September 2024].

45. M. S. Werner, *et al.*, Young genes have distinct gene structure, epigenetic profiles, and transcriptional regulation. *Genome Res* **28**, 1675–1687 (2018).

46. M. M, *et al.*, Evolution of lateralized gustation in nematodes. *bioRxiv : the preprint server for biology* (2025). https://doi.org/10.1101/2024.08.31.610597.

47. R. W. Murray, Electrical Sensitivity of the Ampullæ of Lorenzini. *Nature* **187**, 957–957 (1960).

48. E. O. Gracheva, *et al.*, Molecular basis of infrared detection by snakes. *Nature* **464**, 1006–1011 (2010).

49. C. Procko, *et al.*, Mutational analysis of mechanosensitive ion channels in the carnivorous Venus flytrap plant. *Curr Biol* **33**, 3257-3264.e4 (2023).

50. L. van Giesen, P. B. Kilian, C. A. H. Allard, N. W. Bellono, Molecular basis of chemotactile sensation in octopus. *Cell* **183**, 594-604.e14 (2020).

51. B. M. Olivera, J. Seger, M. P. Horvath, A. Fedosov, Prey-capture Strategies of Fish-hunting Cone Snails: Behavior, Neurobiology and Evolution. *Brain Behav Evol* **86**, 58–74 (2015).

52. W. Shreffler, T. Magardino, K. Shekdar, E. Wolinsky, The unc-8 and sup-40 genes regulate ion channel function in Caenorhabditis elegans motorneurons. *Genetics* **139**, 1261–1272 (1995).

53. C. Cros, O. Hobert, Caenorhabditis elegans sine oculis/SIX-type homeobox genes act as homeotic switches to define neuronal subtype identities. *Proceedings of the National Academy of Sciences* **119**, e2206817119 (2022).

54. R. J. Androwski, *et al.*, Mutually exclusive dendritic arbors in C. elegans neurons share a common architecture and convergent molecular cues. *PLOS Genetics* **16**, e1009029 (2020).

55. H. Lee, *et al.*, Nictation, a dispersal behavior of the nematode Caenorhabditis elegans, is regulated by IL2 neurons. *Nat Neurosci* **15**, 107–112 (2011).

56. I. A. Nikonorova, *et al.*, Isolation, profiling, and tracking of extracellular vesicle cargo in Caenorhabditis elegans. *Curr Biol* **32**, 1924-1936.e6 (2022).

57. J. Wang, *et al.*, Cell-Specific Transcriptional Profiling of Ciliated Sensory Neurons Reveals Regulators of Behavior and Extracellular Vesicle Biogenesis. *Curr Biol* **25**, 3232–3238 (2015).

771 58. P. W. Sternberg, *et al.*, WormBase 2024: status and transitioning to Alliance infrastructure. *Genetics*
772 **227**, iyae050 (2024).

773 59. V. L. Hunt, *et al.*, The genomic basis of parasitism in the Strongyloides clade of nematodes. *Nat*
774 *Genet* **48**, 299–307 (2016).

775 60. M. Dayi, *et al.*, Nearly Complete Genome Assembly of the Pinewood Nematode Bursaphelenchus
776 xylophilus Strain Ka4C1. *Microbiol Resour Announc* **9**, e01002-20 (2020).

777 61. Y.-J. Choi, *et al.*, A Deep Sequencing Approach to Comparatively Analyze the Transcriptome of
778 Lifecycle Stages of the Filarial Worm, Brugia malayi. *PLOS Neglected Tropical Diseases* **5**, e1409
779 (2011).

780 62. J. Foster, *et al.*, The Wolbachia genome of Brugia malayi: endosymbiont evolution within a human
781 pathogenic nematode. *PLoS Biol* **3**, e121 (2005).

782 63. Y. Wang, *et al.*, A glial DEG/ENaC channel functions with neuronal channel DEG-1 to mediate specific
783 sensory functions in C. elegans. *EMBO J* **27**, 2388–2399 (2008).

784 64. P. H. Schiffer, *et al.*, The genome of Romanomermis culicivorax: revealing fundamental changes in
785 the core developmental genetic toolkit in Nematoda. *BMC Genomics* **14**, 923 (2013).

786 65. P. K. Korhonen, *et al.*, Phylogenomic and biogeographic reconstruction of the Trichinella complex.
787 *Nat Commun* **7**, 10513 (2016).

788 66. D. M. Emms, S. Kelly, OrthoFinder: phylogenetic orthology inference for comparative genomics.
789 *Genome Biology* **20**, 238 (2019).

790 67. K. Nakayama, Y. Ishita, T. Chihara, M. Okumura, Screening for CRISPR/Cas9-induced mutations using
791 a co-injection marker in the nematode Pristionchus pacificus. *Dev Genes Evol* **230**, 257–264
792 (2020).

793 68. R Core Team, R: A language and environment for statistical computing.

794

Figure 1

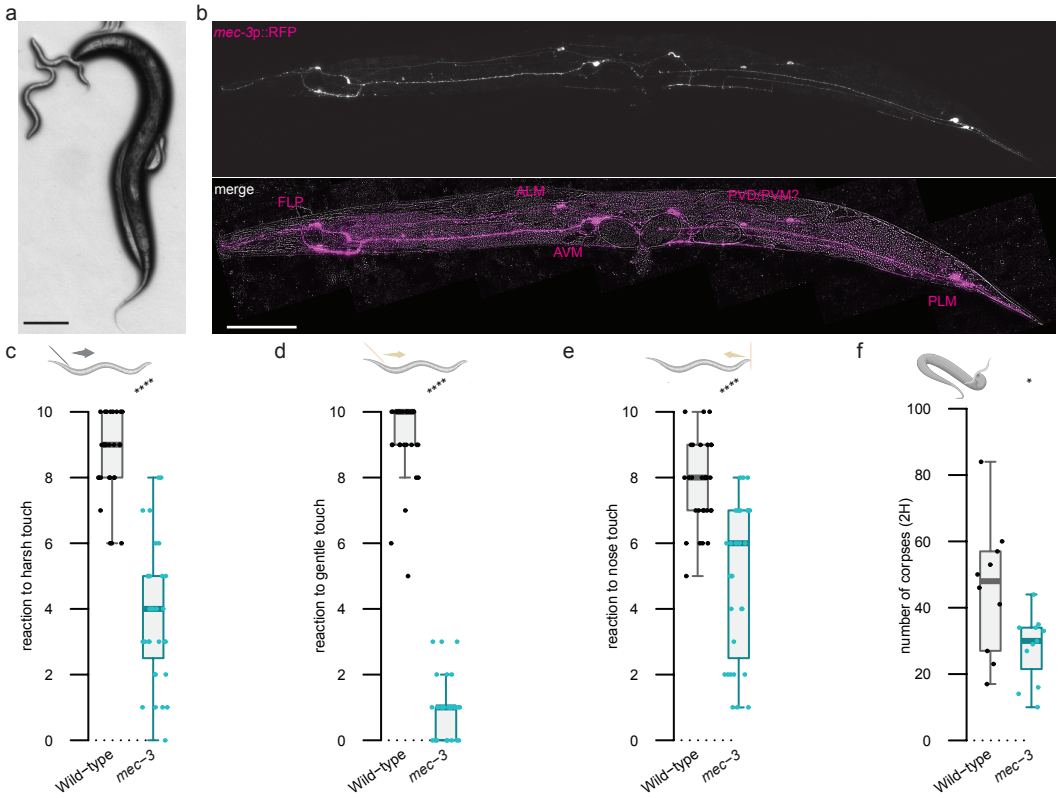
a
b
mec-3p::RFP
merge
FLP
ALM
PVD/PVM?
AVM
PLM
c
d
e
f
****
****
****
*
reaction to harsh touch
reaction to gentle touch
reaction to nose touch
number of corpses (2H)
0
2
4
6
8
10
0
20
40
60
80
100
Wild-type
mec-3

Figure 2

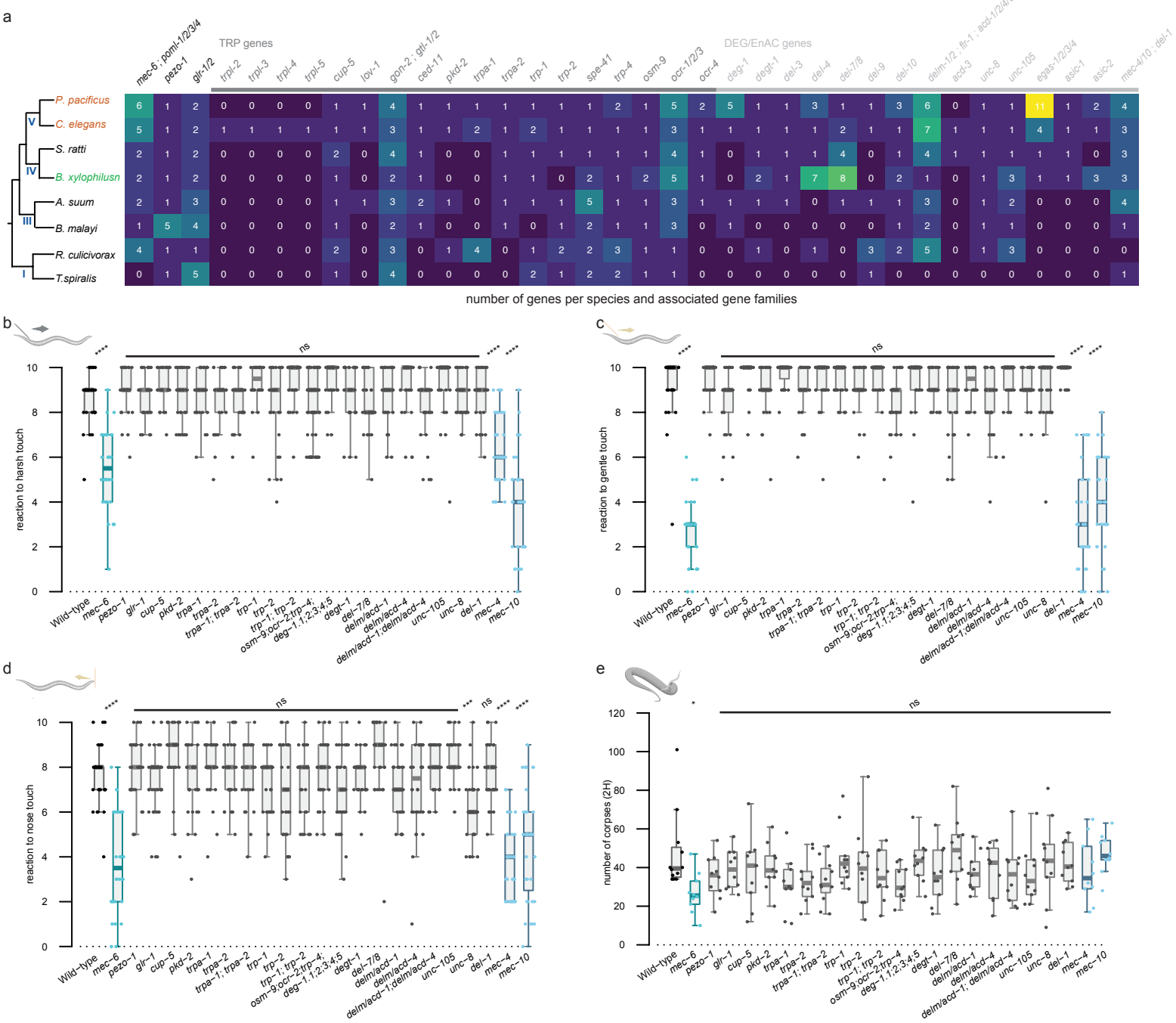
a
TRP genes
DEG/EnAC genes
mec-6 ; pomt-1/2/3/4
pezo-1
glr-1/2
trpl-2
trpl-3
trpl-4
trpl-5
cup-5
lov-1
gon-2 ; gtl-1/2
ced-11
pkd-2
trpa-1
trpa-2
trp-1
trp-2
spe-41
trp-4
osm-9
ocr-1/2/3
ocr-4
deg-1
degt-1
del-3
del-4
del-7/8
del-9
del-10
delm-1/2 ; flr-1 ; acd-1/2/4/5
acd-3
unc-8
unc-105
egas-1/2/3/4
asic-1
asic-2
mec-4/10 ; del-1
P. pacificus
C. elegans
S. ratti
B. xylophilusn
A. suum
B. malayi
R. culicivorax
T.spiralis
V
IV
III
I
number of genes per species and associated gene families
b
reaction to harsh touch
c
reaction to gentle touch
d
reaction to nose touch
e
number of corpses (2H)
ns
Wild-type
mec-6
pezo-1
glr-1
cup-5
pkd-2
trpa-1
trpa-2
trpa-1; trpa-2
trp-1
trp-2
trp-1; trp-2
osm-9;ocr-2;trp-4;
deg-1;2;3;4;5
degt-1
del-7/8
delm/acd-1
delm/acd-4
delm/acd-1;delm/acd-4
unc-105
unc-8
del-1
mec-4
mec-10

Figure 3

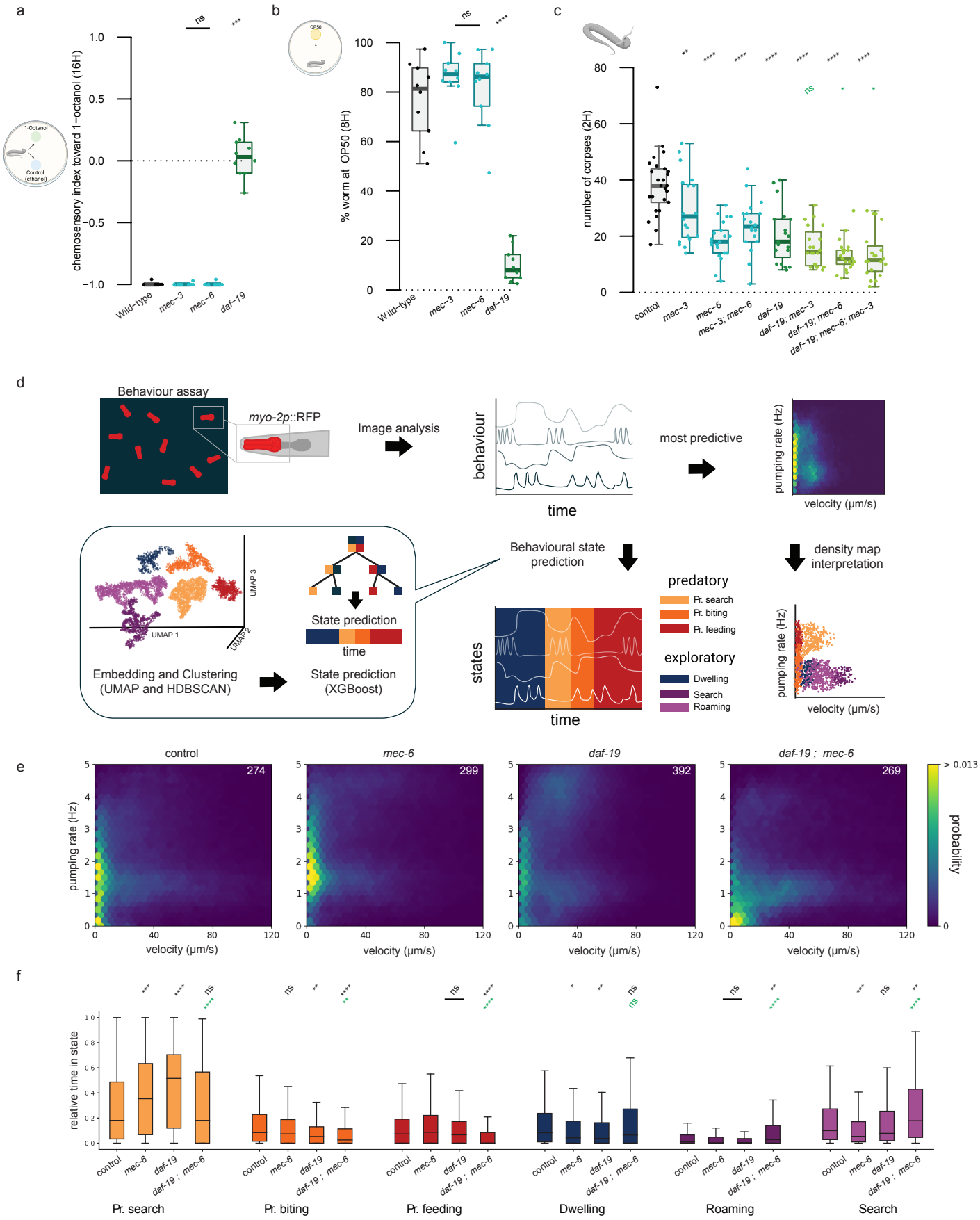
a
1-Octanol
Control (ethanol)
chemosensory index toward 1-octanol (16H)
1.0
0.5
0.0
−0.5
−1.0
ns
***
Wild-type
mec-3
mec-6
daf-19
b
OP50
% worm at OP50 (8H)
100
80
60
40
20
0
ns
****
Wild-type
mec-3
mec-6
daf-19
c
number of corpses (2H)
80
60
40
20
0
**
****
****
****
****
****
****
ns
control
mec-3
mec-6
mec-3; mec-6
daf-19
daf-19; mec-3
daf-19; mec-6
daf-19; mec-6; mec-3
d
Behaviour assay
myo-2p::RFP
Image analysis
behaviour
time
most predictive
pumping rate (Hz)
velocity (μm/s)
UMAP 1
UMAP 2
UMAP 3
Embedding and Clustering
(UMAP and HDBSCAN)
State prediction
time
State prediction
(XGBoost)
Behavioural state
prediction
density map
interpretation
states
time
predatory
Pr. search
Pr. biting
Pr. feeding
exploratory
Dwelling
Search
Roaming
pumping rate (Hz)
velocity (μm/s)
e
control
mec-6
daf-19
daf-19 ; mec-6
274
299
392
269
pumping rate (Hz)
velocity (μm/s)
> 0.013
probability
0
f
relative time in state
control
mec-6
daf-19
daf-19 ; mec-6
Pr. search
Pr. biting
Pr. feeding
Dwelling
Roaming
Search

Figure 4

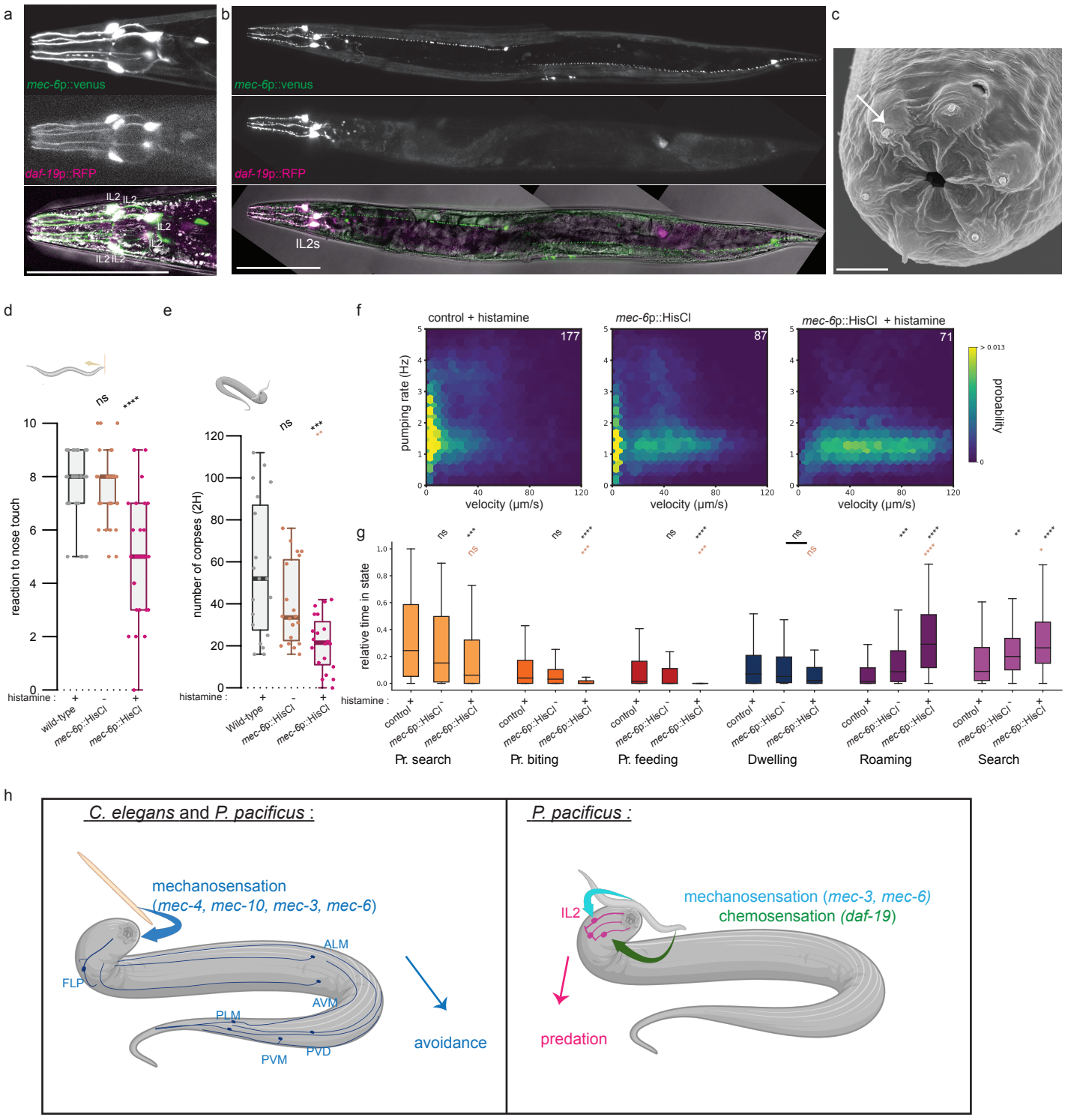
a
mec-6p::venus
daf-19p::RFP
IL2
b
mec-6p::venus
daf-19p::RFP
IL2s
c
d
reaction to nose touch
histamine :
wild-type
mec-6p::HisCl
ns
****
e
number of corpses (2H)
Wild-type
mec-6p::HisCl
ns
***
f
control + histamine
mec-6p::HisCl
mec-6p::HisCl + histamine
177
87
71
pumping rate (Hz)
velocity (µm/s)
probability
> 0.013
g
relative time in state
control
mec-6p::HisCl
Pr. search
Pr. biting
Pr. feeding
Dwelling
Roaming
Search
h
C. elegans and P. pacificus :
mechanosensation
(mec-4, mec-10, mec-3, mec-6)
FLP
ALM
AVM
PLM
PVD
PVM
avoidance
P. pacificus :
IL2
mechanosensation (mec-3, mec-6)
chemosensation (daf-19)
predation